JOURNAL OF MATERIALS SCIENCE **38** (2003) 515–520

Selectivity of metal cations and lithium isotopes on ion exchangers in the hydrogen form prepared by thermal treatment of $NH_4Zr_2(PO_4)_3$

R. KIKUCHI, H. TAKAHASHI, T. OI*
Department of Chemistry, Sophia University, 7-1 Kioicho, Chiyodaku, Tokyo 102-8554, Japan
E-mail: t-ooi@sophia.ac.jp

MORIKAZU HOSOE
Department of Earth and Ocean Sciences, National Defense Academy, 1-10-20 Hashirimizu, Yokosuka, Kanagawa 239-8686, Japan

$NH_4Zr_2(PO_4)_3$ with different particle sizes and different specific surface areas were obtained by controlling the preparation conditions. $HZr_2(PO_4)_3$, cation exchangers in the hydrogen form, were prepared by the thermal treatment of $NH_4Zr_2(PO_4)_3$ in the temperature range of 400 to 700°C and their ion exchange properties were investigated with the main focus on the selectivity for group I and II metal ions and lithium isotopes. Irrespective of the temperature of the thermal treatment, $HZr_2(PO_4)_3$ showed especially high affinity toward the lithium ion, high affinity toward the sodium ion and had little selectivity for the rubidium and cerium ions from the group I metal ions, and showed no specific affinity toward any of group II metal ions. $HZr_2(PO_4)_3$ were isotopically ^{6}Li-specific in any conditions examined. The ^{6}Li-to-^{7}Li isotopic separation factor was nearly independent of temperature of the thermal treatment. It depended, however, on the pH of lithium ion-containing solution used as the solution phase in an ion exchange experiment. This pH dependence of the lithium isotope separation effect was due to the appearance of the $LiZr_2(PO_4)_3$ phase and/or the hydration number of the lithium ion in the ion exchanger phase.

1. Introduction

Ion exchange chromatography is a promising method for large-scale lithium isotope separation. Commercially available organic ion exchangers are generally used as column-packing materials, and the ^{7}Li-to-^{6}Li single-stage separation factor, S, of up to about 1.003 is observed at room temperature [1]. Here, S is defined as

$$S = \frac{(\text{amount of } ^6\text{Li in ion exchanger phase})}{(\text{amount of } ^7\text{Li in ion exchanger phase})} \times \frac{(\text{amount of } ^7\text{Li in solution phase})}{(\text{amount of } ^6\text{Li in solution phase})}.$$

This isotope separation effect is small, compared with those of amalgam [2, 3] and macrocyclic polyether [4] systems, and the development of ion exchangers with large lithium isotope effects is sought to realize efficient chromatographic processes of lithium isotope separation.

It was reported that some inorganic ion exchangers including metal(IV) phosphates exhibited lithium isotope effects several times to an order of magnitude larger than those of organic ion exchangers. In previous papers [5–7], the selectivity of group I metal ions and lithium isotopes on crystalline zirconium and zirconium/titanium phosphates was reported. As those papers and others indicated, there seemed some correlation between the group I metal ion selectivity and lithium isotope selectivity. Inorganic ion exchangers with high affinity toward lithium or sodium ion from the group I metal ions tended to exhibit high lithium isotope selectivity [5–11].

In a recent paper [12], the lithium isotope selectivity of semicrystalline titanium phosphate (scTP) was reported. One of the major findings was that the S values exhibited by thermally treated products of scTP were relatively large and dependent on temperature of the thermal treatment. The results led to the idea that the lithium isotope selectivity of $HZr_2(PO_4)_3$ (HZP), a cation exchanger in the hydrogen form, might be improved by changing the temperature of the thermal treatment of its precursor. HZP was prepared by the thermal treatment of $NH_4Zr_2(PO_4)_3$ (NH_4ZP), the precursor, and NH_4ZP crystallized from aqueous solution under mild conditions [13, 14]. Although the maximum S value of 1.039 was obtained on HZP at 25°C [5], an even larger S value might be expected, if lithium isotope selectivity of HZP was dependent on temperature of the thermal treatment of the precursor such as the case of scTP.

*Author to whom all correspondence should be addressed.

In this paper, the selectivity of cations and lithium isotopes on HZPs prepared by the thermal treatment of two NH_4ZPs with different particle sizes and specific surface areas, obtained by controlling the growth of crystallization from mother solutions, is reported.

2. Experimental

2.1. Preparation of ion exchangers

NH_4ZP was prepared, referring to the method in the literature [13, 14] with some modification. To a mixed solution of oxalic acid and ZrO^{2+}, with the molar ratio of oxalic acid and ZrO^{2+} being 3 : 2, was added NaH_2PO_4 solution until the Zr : P mole ratio became 1 : 0.98. The pH of the mixture was adjusted to 2 with NH_3 and the mixture was allowed to stand at 100°C for 10 days with occasional stirring. The precipitate formed was collected by filtration, washed with excess water and air-dried at room temperature. The product is designated as NH_4ZP-A. A similar synthetic procedure was conducted except that the molar ratio of oxalic acid and ZrO^{2+} was 3.2 : 2 and the pH was 2.5 to obtain another NH_4ZP, hereafter designated as NH_4ZP-B. The particle size of NH_4ZP-B was smaller than that of NH_4ZP-A. Various HZPs were obtained by thermally treating NH_4ZP at different temperatures between 400 and 700°C. Hereafter, HZP obtained by the thermal treatment of NH_4ZP-X at xxx°C is expressed as HZP-X-xxx.

2.2. Characterization

Powder X-ray diffraction (XRD) patterns were recorded with a Rigaku RAD-IIA X-ray diffractometer. Specific surface areas were measured by the BET method with a Microbetrics Flowsorb II2300. Scanning electron microscopic (SEM) photographs were taken with a Hitachi S-4500 electron microscope, and infrared (IR) spectra were obtained with a Perkin Elmer 1650 IR spectrometer. Thermogravimetry (TG) and differential thermal analysis (DTA) were carried out with a Rigaku TAS-200 TG-DTA analyzer, and identification and monitoring of gases released during TG measurements (TG-IR) were done with an apparatus consisting of a Perkin Elmer Spectrum 2000 IR spectrometer and a Perkin Elmer TGA7 TG analyzer.

2.3. Cations and lithium isotopes selectivity

To examine the selectivity of group I and II metal ions, the distribution coefficient, K_d, in cm^3/g was calculated using,

$$K_d = \frac{\text{amount of cation in 1 g solid phase}}{\text{amount of cation in 1 cm}^3\text{ solution phase}}.$$

Approximately 0.1 g of ion exchanger was weighed out accurately, and put in 10 cm^3 of ammonia-ammonia chloride buffer solution of pH 9.18 containing Li^+, Na^+, K^+, Rb^+, Cs^+, Mg^{2+}, Ca^{2+}, Sr^{2+} and Ba^{2+} ions of 1.0 mM (1 M = 1 mol/dm^3), and the solution was allowed to stand at 25°C for 7 days. After equilibrium was attained, the solid phase was separated from the solution phase by filtration. The concentrations of group I metal ions in the solution phase were determined flame photometrically and those of group II elements with an ICP spectrometer. The amount of a cation in the solid phase was calculated from the concentration difference before and after the equilibration.

The S values for the lithium isotope selectivity were obtained in batch experiments, as summarized in Table I. Approximately 0.15 g of ion exchanger was weighed out accurately, put in 5.0 cm^3 of 0.10 M of lithium hydroxide solution, and the solution was allowed to stand at 25°C for 7 days. The solid phase was then separated from the solution phase by filtration, and the lithium concentration of the solution phase was measured. The $^7Li/^6Li$ isotopic ratio of the solution phase was measured by the surface ionization technique with a Finnigan Mat 261 mass spectrometer or a Varian Mat CH-5 mass spectrometer. From the experimental data from the solution phase, S was calculated using the following equation,

$$S = [r(1+r)C_0 - r(1+r_0)C]/[r_0(1+r)C_0 - r(1+r_0)C],$$

where C_0 and C were the lithium concentrations before and after equilibration and r_0 and r were the lithium isotopic ratios before and after equilibration, respectively. The lithium ion uptake (mmol/g) was also calculated using the weight of the ion exchanger used and the concentration difference before and after the ion exchange equilibrium. Furthermore, the concentration of phosphorus in the solution phase after equilibrium was established was measured with the ICP spectrometer to estimate the degree of decomposition of the ion exchanger used.

Similar experiments were carried out using approximately 0.2 g of the ion exchanger and 5.0 cm^3 of 0.10 M lithium acetate solution and approximately 0.7 g of the ion exchanger and 5.0 cm^3 of 0.10 M lithium chloride solution.

3. Results and discussion

3.1. Characterization

$NH_4Zr_2(PO_4)_3$ with different particle sizes and specific surface areas, NH_4ZP-A and NH_4ZP-B, were synthesized by controlling the preparation conditions. The SEM photographs of NH_4ZP-A and NH_4ZP-B are shown in Fig. 1. The particle sizes of NH_4ZP-A and NH_4ZP-B are about 1 μm and 0.4 μm, respectively, and correspondingly, their specific surface areas are 2.2 and 5.6 m^2/g, respectively. No difference in peak positions in the XRD patterns, however, is detected between the two NH_4ZPs. The XRD pattern of NH_4ZP-A is shown in Fig. 2a and it is in good agreement with that of rhombohedral $NH_4Zr_2(PO_4)_3$ in the literature (JCPDS No. 38-3). No impurity peak is observed.

TG-IR and TG-DTA measurements of NH_4ZP-A up to 900°C show that, with heating NH_4ZP, dehydration occurs in the temperature range 100 to 300°C, NH_4ZP changes into HZP with the release of NH_3 [15] between 300 and 700°C, and condensation of phosphate groups occurs between 640 and 900°C. Based on this thermal behavior of NH_4ZP, the temperatures of the thermal treatment of NH_4ZP were set at 400, 500, 600 and 700°C. It takes 200, 15, 3 and 3 hours to complete the conversion of NH_4ZP into HZP at 400, 500,

TABLE I Experimental conditions and results on lithium isotope selectivity at 25°C

Entry	Ion exchanger	Solution phase[a]	pH[b]	Li^+ ion uptake (mmol/g)		S	
					Average		Average
1	HZP-A-400	0.1 M LiOH	11.47	2.38	2.39	1.019	1.018
2			11.48	2.40		1.016	
3		0.1 M CH_3COOLi	3.78	1.64	1.66	1.026	1.027
4			3.80	1.67		1.028	
5		0.1 M LiCl	1.07	0.378	0.385	1.045	1.047
6			1.06	0.391		1.048	
7	HZP-A-500	0.1 M LiOH	11.54	2.04	2.04	1.023	1.022
8			11.65	2.03		1.020	
9		0.1 M CH_3COOLi	3.71	1.69	1.68	1.032	1.032
10			3.71	1.67		1.032	
11		0.1 M LiCl	1.06	0.623	0.626	1.037	1.036
12			1.06	0.628		1.034	
13	HZP-A-600	0.1 M LiOH	11.41	1.89	1.89	1.030	1.030
14			11.43	1.88		1.029	
15		0.1 M CH_3COOLi	3.82	1.60	1.61	1.031	1.031
16			3.82	1.61		1.030	
17		0.1 M LiCl	1.06	0.632	0.634	1.039	1.039
18			1.07	0.635		1.039	
19	HZP-A-700	0.1 M LiOH	11.26	1.29	1.28	1.022	1.022
20			11.27	1.26			
21		0.1 M CH_3COOLi	4.84	0.284	0.27	1.023	1.024
22			4.78	0.259		1.025	
23		0.1 M LiCl	1.39	0.134	0.129	1.047	1.040
24			1.44	0.123		1.032	
25	HZP-B-500	0.1 M LiOH	11.05	2.32	2.23	1.026	1.027
26			10.99	2.22		1.028	
27	HZP-B-600	0.1 M LiOH	11.13	2.08	2.08	1.028	1.027
28			11.18	2.07		1.026	

[a]Original composition.
[b]The value after Li^+ ion uptake.

600 and 700°C, respectively. The conversion is monitored by the fade-out of the NH_4^+ deformation mode at 1430 cm^{-1} and the appearance of the OH stretching mode at 3460 cm^{-1} in the IR spectra.

The XRD patterns of HZP-A obtained at 400, 500, 600 and 700°C are depicted in Fig. 2b to e, respectively. In spite of small variations in relative peak heights and peak positions, they all agree with the pattern of the rhombohedral $HZr_2(PO_4)_3$ in the literature (JCPDS No. 38-4). It is observed that crystallinity decreases with increasing temperature above 500°C. This is probably attributable to the development of the amorphous state due to partial condensation of phosphate groups. At even higher temperature, the $Zr_4P_6O_{23}$ phase appears, which shows no ion exchange property.

Fig. 3a shows the lattice constants, a and c, of NH_4ZP and HZP as a function of temperature of the thermal treatment. Upon conversion from NH_4ZP to HZP, the a value increases and the c value decreases, and both are nearly independent of temperature of the thermal treatment and also of preparation conditions of the precursor (NH_4ZP-A or NH_4ZP-B). Fig. 3b, in which the specific surface area is plotted against temperature of the thermal treatment, shows that the thermal treatment has no substantial effect on the specific surface area of HZP.

3.2. Ion and lithium isotope selectivity

Logarithms of K_d values are plotted against the temperature of the thermal treatment in Fig. 4a (for HZP-A) and b (for HZP-B). The lithium ion K_d values are above the detection limit of the apparatus indicating that they must be 50,000 or larger. The decreasing order of the K_d value of group I elements at pH = 9.18 is $Li^+ \gg Na^+ \gg K^+ > Rb^+ \approx Cs^+$. HZP is thus lithium ion-specific from the group I metal ions, shows relatively high affinity toward the sodium ion, but shows little affinity toward rubidium and cesium ions, which is in good agreement with the results of the previous paper [5]. These features are nearly independent of temperature of the thermal treatment. Those results indicate that the size of the ion exchange site of HZP is best fitted to the lithium ion and too small for potassium and larger ions and is little altered by temperature of the thermal treatment. The latter is consistent with the lattice constants shown in Fig. 3a. HZP shows little specific affinity toward any of the group II elements examined. The $\log K_d$ value of the magnesium ion contrasts strikingly with that of the lithium ion in spite of the similarity in their ionic radii (71 and 73 pm for the Mg^{2+} and Li^+ ions, respectively, with the coordination number being 4 [16]). This difference is most probably attributable to the difference in standard Gibbs energy of hydration between the two ions; −1904 kJ/mol for Mg^{2+} vs. −510.4 kJ/mol for Li^+ [17]. Due to its relatively small standard Gibbs energy of hydration, hydrated lithium ions in aqueous solution can be dehydrated upon ion exchange with protons in HZP and can enter the HZP particles, while magnesium ions in aqueous solution are too strongly hydrated to be dehydrated. A close comparison of Fig. 4a and b reveals that HZP-B, with a smaller particle size, has slightly larger affinity toward potassium and barium ions than HZP-A.

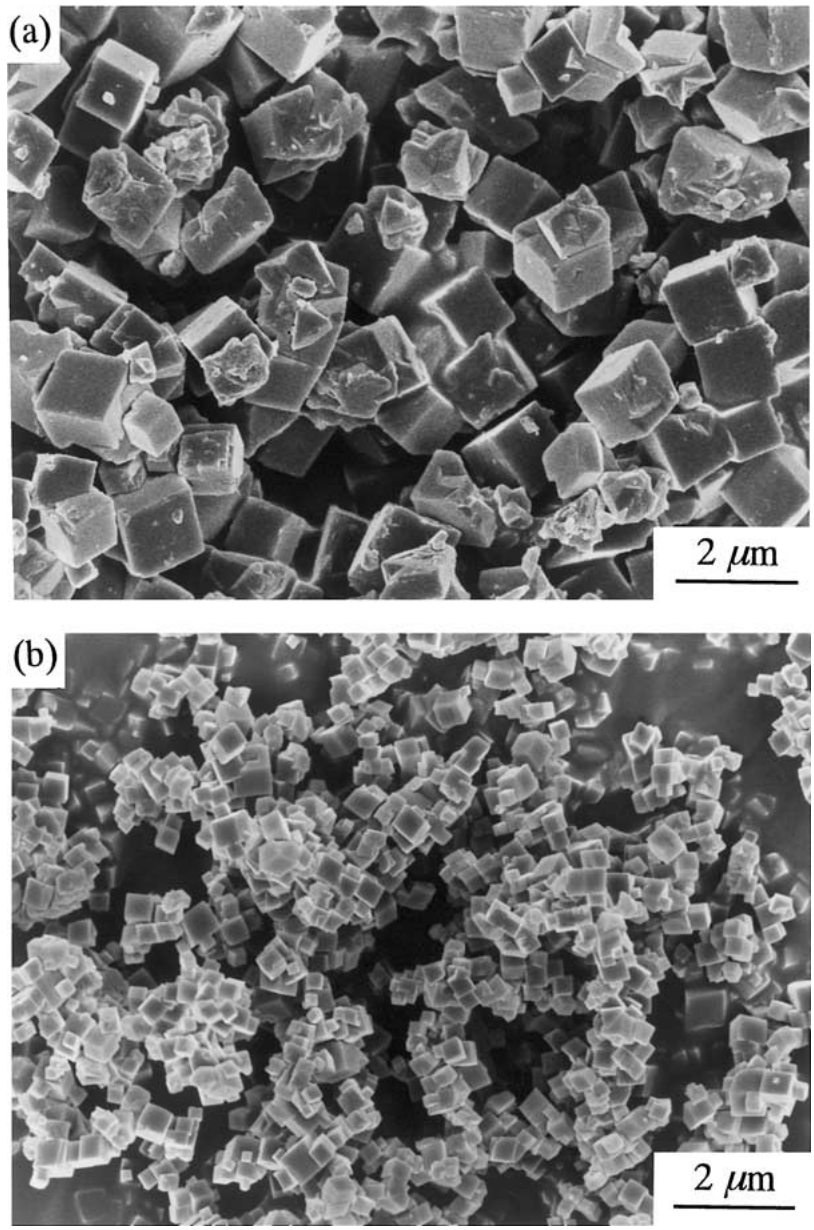

Figure 1 SEM photographs of (a) NH_4ZP-A and (b) NH_4ZP-B.

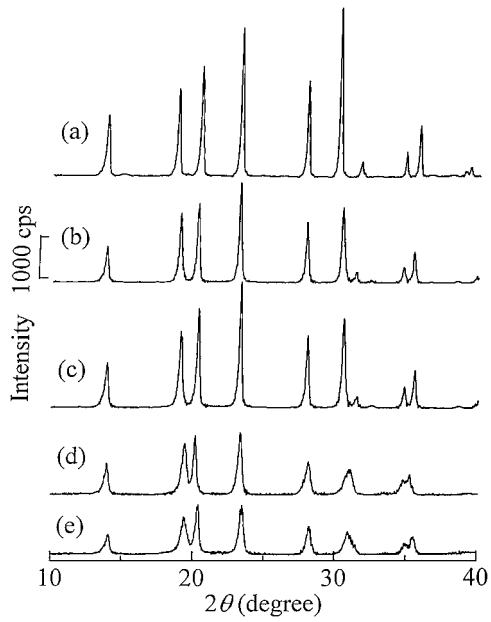

Figure 2 XRD patterns of (a) NH_4ZP-A, (b) HZP-A-400, (c) HZP-A-500, (d) HZP-A-600 and (e) HZP-A-700.

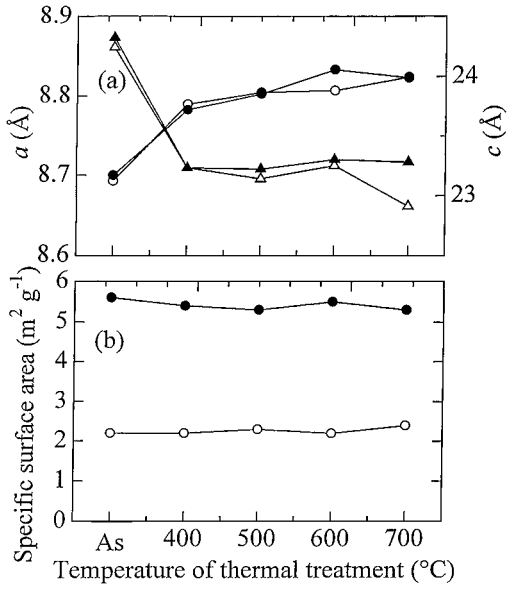

Figure 3 (a) lattice constants, a(○, ●) and c(△, ▲), and (b) specific surface area as a function of temperature of the thermal treatment of NH_4ZP-A (○) and NH_4ZP-B (●) with As meaning "as prepared".

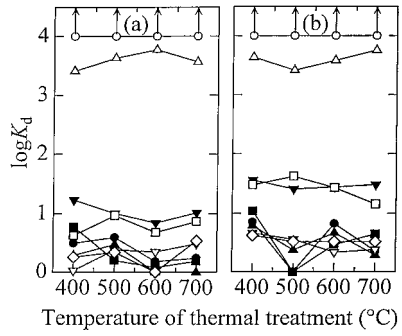

Figure 4 Plots of distribution coefficients (K_d) of Li^+ (○), Na^+ (△), K^+ (□), Rb^+ (▽), Cs^+ (◊), Mg^{2+} (●), Ca^{2+} (▲), Sr^{2+} (■) and Ba^{2+} (▼) on (a) HZP-A and (b) HZP-B against temperature of the thermal treatment with the arrows indicating that the K_d values of the lithium ion are out of the frames.

HZP-B has the larger specific surface area and thus has the larger amount of exchange sites on the surface of particles than HZP-A, which accounts for the slightly different ion exchange properties between the two ion exchangers.

The lithium ion uptake is summarized in Table I. For a given ion exchanger, the lithium ion uptake from lithium hydroxide solution is largest, that from lithium chloride solution is the smallest and that from the lithium acetate solution is in between. This sequence is the same as the decreasing order of pH of the solution after equilibration. Thus, the effective ion exchange capacity of HZP is larger at a higher pH. For a given solution phase, the lithium ion uptake of HZP obtained at 700°C is smaller than those of HZPs obtained at lower temperatures. This is consistent with the development of the amorphous state caused by the partial condensation of phosphate groups mentioned above.

Specific surface areas of HZP-Bs after ion exchange equilibrations with lithium hydroxide, lithium acetate and lithium chloride solutions are plotted against pH of solution in Fig. 5. Also plotted is the degree of decomposition of the HZP-Bs, due to the hydrolysis of phosphate groups, as calculated from the concentration of phosphorus in the solution phase. In cases where the solutions are acidic (lithium acetate and lithium chloride solutions), neither the increase in specific surface area nor the hydrolysis of phosphate groups is observed.

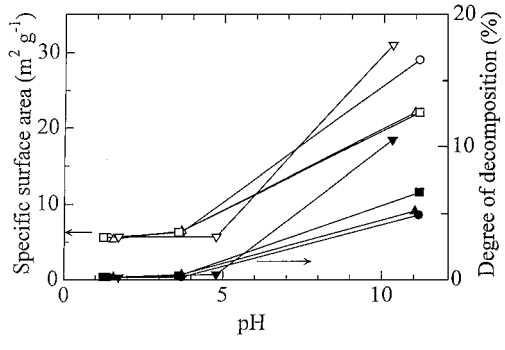

Figure 5 Specific surface areas of HZP-B-400 (○), HZP-B-500 (△), HZP-B-600 (□) and HZP-B-700 (▽) and degree of decomposition (%) of HZP-B-400 (●), HZP-B-500 (▲), HZP-B-600 (■) and HZP-B-700 (▼) as a function of the pH of lithium ion-containing solution after ion exchange.

Contrary to this, 5 to 10% of phosphorus of the ion exchanger is found to be dissolved in the solution phase and the specific surface areas become four to five times larger in lithium hydroxide solution. Thus, in basic solution, phosphate groups of HZP are hydrolyzed and, as a result, the specific surface area increases.

The values of S at 25°C are summarized in the last two columns of Table I. All the values are larger than unity, ranging from 1.018 to 1.047, which means that HZP is isotopically ^{6}Li-specific under the experimental conditions examined. The following observations are made:

(1) For lithium hydroxide solution, no substantial difference in S value is observed between HZP-A and HZP-B.

(2) The temperature of the thermal treatment has no substantial effect on the S value.

(3) For a given ion exchanger (HZP-A or HZP-B), S seems to depend on the pH of the solution; a higher pH results in a smaller S value.

Thus, contrary to the case of semicrystalline titanium phosphate [12] and against expectation, hardly any dependence of S on temperature of the thermal treatment is observed. The lithium isotope effect on HZP is not influenced by particle size, specific surface area or the temperature of the thermal treatment. The observation (3) above is consistent with the results of the previous paper [5].

As has been shown previously [1], varying the counterion to the lithium ion in the solution phase changes the value of $S - 1$ only by about 1×10^{-4} at 25°C when the concentration of the lithium ion is 0.1 M or so. The pH dependence of S is thus ascribable in most part to the ion exchange phase. In Fig. 6, the S value of HZP-A is plotted against the ratio of lithium ion uptake to the theoretical ion exchange capacity (uptake/capacity ratio). In the figure, the data for HZP-A-700 are omitted, since it is impossible to estimate its theoretical ion exchange capacity due to the fact the partial condensation of phosphate groups occurs at 700°C and the degree of the condensation cannot be estimated. As can be seen in the figure, a negative correlation is observed between S and the uptake/capacity ratio. This is consistent with previous results [5], which pointed out that, with increasing lithium ion uptake, the

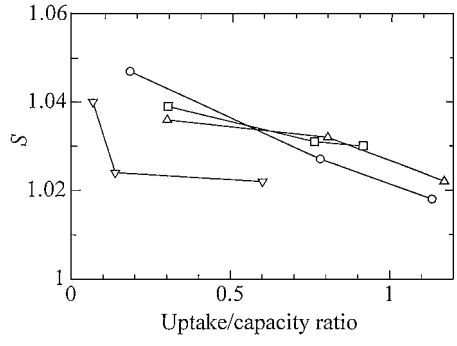

Figure 6 Single-stage separation factor for the lithium isotopes (S) exhibited by HZP-A-400 (○), HZP-A-500 (△), HZP-A-600 (□) and HZP-A-700 (▽) as a function of the uptake/capacity ratio.

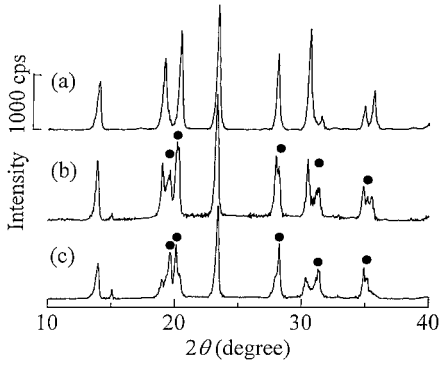

Figure 7 XRD patterns of HZP-A-500 after the lithium ion uptake from (a) lithium chloride solution, (b) lithium acetate solution and (c) lithium hydroxide solution with the peaks of the $LiZr_2(PO_4)_3$ phase marked with ●.

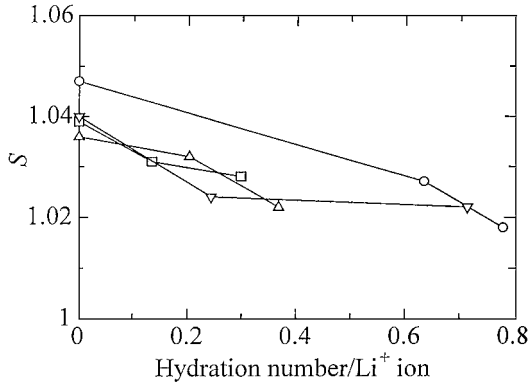

Figure 8 Single-stage separation factor for the lithium isotopes (S) exhibited by HZP-A-400 (○), HZP-A-500 (△), HZP-A-600 (□) and HZP-A-700 (▽) as a function of hydration number of the lithium ion in the ion exchanger phase.

monoclinic $LiZr_2(PO_4)_3$ phase (JCPDS No. 44-10) appeared, which resulted in a decrease in S value, because the lithium isotope effect between the solution phase and the monoclinic phase is expected to be smaller than that between the solution phase and the rhombohedral phase. A similar tendency is observed in these results. In Fig. 7, the XRD patterns of HZP-A-500 after lithium ion uptake from lithium hydroxide, lithium acetate and lithium chloride solutions are shown. When the solution phase is lithium chloride solution, the lithium ion uptake is low (uptake/capacity ratio = 0.13), the $LiZr_2(PO_4)_3$ phase is not observed, and accordingly the S value is relatively large.

An alternative explanation is possible for the pH dependence of the S value. In Fig. 8, the S value is plotted against the hydration number of the lithium ion, $(HN)_{Li}$, in the ion exchanger phase. The hydration number is estimated by the equation:

$$(HN)_{Li} = \frac{1}{MW_{H_2O} \times \text{uptake} \times W_{after}} \times \left(WL_{after} - WL_{before} \times \frac{W_{after}}{W_{before}} \times \frac{C_{theo} - \text{uptake}}{C_{theo}} \right),$$

where MW_{H_2O} is the molecular weight of water (g/mol), uptake is the uptake of the lithium ion (mmol/g), C_{theo} the theoretical ion exchange capacity (mmol/g), W_{before} and WL_{before} are the weight of the ion exchanger submitted to the TG measurement and the weight loss (mg) between 100 and 250°C in that measurement, respectively, and W_{after} and WL_{after} are the weight of the lithium ion-inserted ion exchanger submitted to the TG measurement and the weight loss (mg) between 100 and 250°C in that measurement, respectively. In using the above equation, it is assumed that the weight loss between 100 and 250°C is solely due to the loss of water molecules hydrated to hydrogen and/or lithium ions and that the hydration number of a proton does not change before and after ion exchange equilibration (lithium ion uptake). As is seen, the S value decreases with increasing hydration number of the lithium ion in the ion exchanger phase for every ion exchanger examined. Thus, the present separation factor data can also be elucidated on the basis of the difference in hydration circumstances of the lithium ion between the solution and ion exchanger phases, as has been pointed out previously [8, 9].

4. Conclusion

In summary, by controlling the preparation conditions of the precursor, NH_4ZP, the particle size and specific surface area of HZP can be controlled to some extent. However, the difference in preparation conditions of HZP does not result in substantial changes in cation selectivity or lithium isotope selectivity. The maximum S value is 1.047 at 25°C, which suggests that HZP may be a promising alternative to organic ion exchangers for ion exchange chromatographic lithium isotope separation processes.

References

1. T. OI, K. KAWADA, M. HOSOE and H. KAKIHANA, *Sep. Sci. Technol.* **26** (1991) 1353, and references cited therein.
2. A. A. PALKO, J. S. DRURY and G. M. BEGUN, *J. Chem. Phys.* **64** (1976) 1828.
3. M. FUJIE, Y. FUJII, M. NOMURA and M. OKAMOTO, *J. Nucl. Sci. Technol.* **23** (1986) 330.
4. K. NISHIZAWA and T. TAKANO, *Sep. Sci. Technol.* **23** (1988) 751 and references cited therein.
5. T. OI, Y. UCHIYAMA, M. HOSOE and K. ITOH, *J. Nucl. Sci. Technol.* **36** (1999) 1064.
6. H. TAKAHASHI, T. MIYAJIMA and T. OI, *ibid.* **39** (2002) 463.
7. H. TAKAHASHI and T. OI, *J. Mater. Sci.* **36** (2001) 1621.
8. K. OOI, Q. FENG, H. KANOH, T. HIROTSU and T. OI, *Sep. Sci. Technol.* **30** (1995) 3761.
9. Y. INOUE, Y. KANZAKI and M. ABE, *J. Nucl. Sci. Technol.* **33** (1996) 671.
10. T. OI, K. SHIMIZU, S. TAYAMA, Y. MATSUNO and M. HOSOE, *Sep. Sci. Technol.* **34** (1999) 805.
11. Y. MAKITA, H. KANOH, T. HIROTSU and K. OOI, *Chem. Lett.* (1998) 77.
12. Y. UCHIYAMA, H. TAKAHASHI, T. OI and M. HOSOE, *J. Nucl. Sci. Technol.* **38** (2001) 85.
13. DAIICHI KIGENSO CHEM. IND. CO., *Japan Patent*, 6-53566, 25 (1994) (in Japanese).
14. DAIICHI KIGENSO CHEM. IND. CO., *Japan Patent*, 7-115851, 55 (1995) (in Japanese).
15. T. OI, K. HORIO, R. KIKUCHI and H. TAKAHASHI, *J. Therm. Anal. Cal.* **65** (2001) 305.
16. J. E. HUHEEY, "Inorganic Chemistry," 3rd ed. (Harper & Row, Cambridge, 1983) p. 74.
17. H. OHTAKI, "Ion no suiwa (Hydration of Ions)" (Kyoritsu, Tokyo, 1990) p. 30 (in Japanese).

Received 12 February
and accepted 2 October 2002